

REPORT DOCUMENTATION PAGE				Form Approved OMB No. 0704-0188	
<p>The public reporting burden for this collection of information is estimated to average 1 hour per response, including the time for reviewing instructions, searching existing data sources, gathering and maintaining the data needed, and completing and reviewing the collection of information. Send comments regarding this burden estimate or any other aspect of this collection of information, including suggestions for reducing the burden, to Department of Defense, Washington Headquarters Services, Directorate for Information Operations and Reports (0704-0188), 1215 Jefferson Davis Highway, Suite 1204, Arlington, VA 22202-4302. Respondents should be aware that notwithstanding any other provision of law, no person shall be subject to any penalty for failing to comply with a collection of information if it does not display a currently valid OMB control number.</p> <p>PLEASE DO NOT RETURN YOUR FORM TO THE ABOVE ADDRESS.</p>					
1. REPORT DATE (DD-MM-YYYY)	2. REPORT TYPE			3. DATES COVERED (From - To)	
11/27/2012	Final Report			From 5-1-2010 - To 09-30-2012	
4. TITLE AND SUBTITLE Ferrite-Ferroelectric Heteroepitaxial Structures and Frequency Agile Multiferroic RF Components				5a. CONTRACT NUMBER	
				5b. GRANT NUMBER	N00014-10-1-0696
				5c. PROGRAM ELEMENT NUMBER	
6. AUTHOR(S) Gopalan Srinivasan				5d. PROJECT NUMBER	12PR02117-01
				5e. TASK NUMBER	
				5f. WORK UNIT NUMBER	
7. PERFORMING ORGANIZATION NAME(S) AND ADDRESS(ES) Oakland University Rochester MI 48309				8. PERFORMING ORGANIZATION REPORT NUMBER	
9. SPONSORING/MONITORING AGENCY NAME(S) AND ADDRESS(ES) Office of Naval Research 875 North Randolph Street Arlington VA 22230-1995				10. SPONSOR/MONITOR'S ACRONYM(S) ONR- code 312	
				11. SPONSOR/MONITOR'S REPORT NUMBER(S)	
12. DISTRIBUTION/AVAILABILITY STATEMENT Approved for Public Release - distribution is Unlimited					
13. SUPPLEMENTARY NOTES					
14. ABSTRACT Results of our ONR supported activities on miniature, rapid-response, frequency agile multiferroic RF components are discussed here. Ferrite-ferroelectric bilayers were synthesized by techniques including electrophoretic deposition, eutectic bonding and MOCVD and were characterized in terms of strain mediated magneto-electric coupling by ferromagnetic resonance. Devices studied include 1-3GHz ferrite-ferroelectric band-pass filter, 18-36 GHz magneto-dielectric band-pass filter, 12-24 GHz hexaferrite-ferroelectric phase shifter and beam-forming antennas.					
15. SUBJECT TERMS					
16. SECURITY CLASSIFICATION OF:		17. LIMITATION OF ABSTRACT	18. NUMBER OF PAGES	19a. NAME OF RESPONSIBLE PERSON 19b. TELEPHONE NUMBER (Include area code)	
a. REPORT	b. ABSTRACT	c. THIS PAGE			

FINAL REPORT

**Ferrite-Ferroelectric Heteroepitaxial Structures and Frequency Agile
Multiferroic RF Components
(N00014-10-1-0696)**

Period of Performance: May 1, 2008 – September 30, 2012

Principal Investigator

Gopalan Srinivasan
Distinguished Professor
Physics Department
Oakland University
Rochester, MI 48309

Phone: (248) 370-3419
Email: srinivas@oakland.edu

20121203003

Summary

Results of our ONR supported activities on miniature, rapid-response, frequency agile multiferroic RF components are discussed here. When a ferrite-ferroelectric composite is subjected to an electric field E , the mechanical deformation due to piezoelectric effect manifests as a *frequency* shift in the spin wave spectrum or ferromagnetic resonance (FMR) for the ferrite. The traditional *magnetic field* tuning of FMR based ferrite devices is slow, noisy, and requires large power. In contrast, E -tuning is much faster, less noisy, and has practically zero power consumption. Such devices can easily be miniaturized and integrated with semiconductor devices.

Our key accomplishments under this program are as follows.

Materials:

- (1) Growth of ferrite films on piezoelectric substrates by electrophoretic deposition techniques: Studies focused on 1-10 μm thick polycrystalline YIG films on PZT. The strength of magneto-electric (ME) interactions measured over 1-40 GHz was comparable to results for bilayers of single crystal LPE YIG films-PZT.
- (2) Eutectic bonding techniques for ferrite-piezoelectric bilayer synthesis: Samples of YIG/PMN-PT and hexagonal ferrite/PMN-PT showed an order of magnitude stronger ME coupling compared to epoxy bonded samples.
- (3) Heterostructures of nickel ferrite films on PMN-PT (grown by MOCVD-collaborative effort with Dr. Gupta, University of Alabama): The samples showed ME coupling on the order of 25 MHz cm/kV. But the ferromagnetic resonance line-width was on the order of 200-500 Oe. Line-width reduction is a key requirement for device applications.

Devices:

- (4) 10-24 GHz Phase shifter: Eutectic bonded hexagonal Zn₂Y ferrite and PMN-PT was used for E-tunable ferrite phase shifter. Low insertion loss and linear control of the phase shift with E were achieved.
- (5) 1-3 GHz band-pass filter: YIG-PZT bandpass filter showed insertion loss of 1-3 dB and E-tuning by 10%.
- (6) 18-36 GHz magneto-dielectric band-pass filter: A polycrystalline nickel ferrite was used to achieve a filter based on dielectric resonance. The filter could be tuned with a magnetic field and had low insertion loss.
- (7) Multiferroic beam-forming antennas: Studies were performed on voltage control of the radiation pattern with the use of YIG-PZT bilayers in a π -type antenna.

Studies to-date also point to the following challenges in the figures of merit: (i) limited tuning range of $\sim 1\text{-}10\%$; (ii) non-linear voltage tuning (due to non-linear piezoelectric deformation in ferroelectrics); and (iii) poor power handling (~ 10 mW) due to spin wave instabilities in devices based on single crystal YIG films.

There are several avenues to rectify the above problems and unlock the potential in multiferroic RF components for novel devices such as a tunable radar!

Table of Contents

SF 298	1
Cover page	2
Summary	3
Table of contents	4
1. Electrophoretic Deposition of YIG films on PZT	5
2. Eutectic bonding techniques for ferrite-piezoelectric bilayer synthesis	6
3. MOCVD grown nickel ferrite/PMN-PT	7
4. Zn ₂ Y/PMN-PT 10-24 GHz Phase shifter	7
5. YIG-PZT 1-3 GHz Band-pass Filter	8
6. A magneto-dielectric band-pass filter for 18-36 GHz	9
7. Multiferroic beam-forming antennas	9
6. Concluding remarks	10
Appendix I: Publications	11

1. Electrophoretic Deposition of YIG films on PZT

Electrophoretic deposition (EPD) is a powerful tool for the deposition of oxides, metals, and composites. Our work focused on a layered multiferroic structure obtained by the EPD deposition of YIG films on PZT and (001) PMN-PT. YIG nano particles synthesized by coprecipitation techniques were used for the deposition of films of thickness 10-100 μm . The bilayer thus obtained was used in a microstripline for microwave ME studies.

The powders of YIG ($\text{Y}_3\text{Fe}_5\text{O}_{12}$) were prepared by the coprecipitation technique by dissolving $\text{Y}(\text{NO}_3)_3 \cdot 6\text{H}_2\text{O}$ and $\text{Fe}(\text{NO}_3)_3 \cdot 9\text{H}_2\text{O}$ with $[\text{Fe}^{3+}]/[\text{Y}^{3+}] = 5/3$, into an ammoniacal solution of $\text{pH} = 10$. The obtained precipitate was washed several times with deionized water and ethanol, filtered and dried at 65°C for 24 h. The powders were then calcined at 1200°C to form fine garnet particles.

In EPD particles dispersed or suspended in a liquid medium get deposited under the influence of a DC electric field (electrophoresis), forming a relatively dense and homogeneously compact film. The EPD was performed in a cell with two electrodes (5 mm apart) vertically immersed in a solvent media. The solvent media (Ethanol (150ml), PVB (1mg) and Phosphate Ester) is stirred by magnetic stirrer for 30 min. The pH of the suspension is maintained at 3.5. Then 1 g of YIG nano particles was introduced into the cell. Electrophoretic deposition was carried out for 90 min at a constant voltage condition of 25 V. The obtained deposits were dried in air at room temperature. In order to support higher annealing temperatures, Titanium (15nm) – Platinum (500nm) are deposited on both sides of the PZT samples. The deposited thin films are annealed at 1050°C .

A $6\mu\text{m}$ film was fabricated by EPD at a deposition rate of 400 nm/min. Figure 1 shows AFM surface profile of the film. The films were found to be composed of large particles of 150–200 nm size, whereas the size of particles in the starting solution was in the range 10–20 nm. It is considered that the particles undergo agglomeration during deposition. FMR data were typical of polycrystalline film with a line-width $\Delta H = 50$ Oe. Figure 2 shows E-tuning of FMR. The strength of ME interactions $A = \delta f/E \sim 1.5$ MHz cm/kV which is comparable to values for epoxy bonded LPE YIG and PZT.

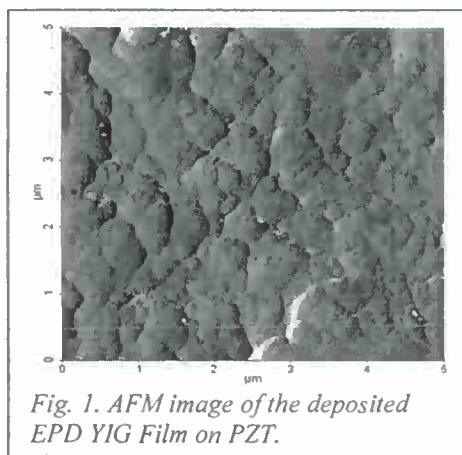


Fig. 1. AFM image of the deposited EPD YIG Film on PZT.

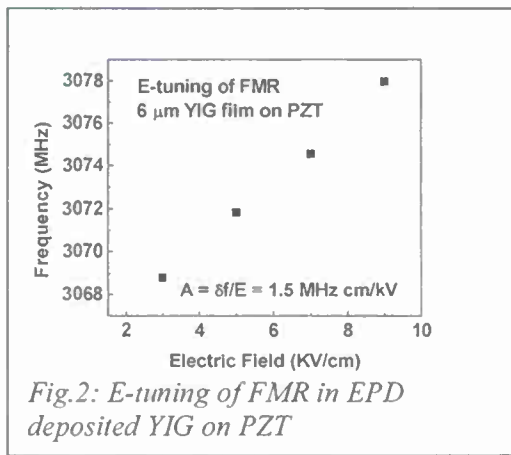


Fig. 2: E-tuning of FMR in EPD deposited YIG on PZT

Reference: "Broadband Ferromagnetic Resonance Studies on Influence of Interface Bonding on Magnetoelastic Effects in Ferrite-Ferroelectric Composites," D.V.B.Murthy and G. Srinivasan, *Frontiers in Physics*, 7, 418 (2012).

2. Eutectic bonding techniques for ferrite-piezoelectric bilayer synthesis

2.1: YIG/PZT/PMN-PT: For eutectic bonding, a thin layer (100-300 nm) of silicon was deposited onto YIG by rf sputtering and 100 nm thick silver on PZT or PMN-PT. The bilayer was then placed in a furnace, subjected to a nominal pressure and heated to 600 C. After the high temperature treatment the sample was poled at room temperature.

Figure 3 shows E-tuning data on δf vs E for a bilayer in which the Si layer was 100 nm in thickness. The ME coefficient A estimated from the data is 2.2 MHz cm/kV which is 50% higher than for epoxy bonded for YIG-PZT. Samples with 300 nm and 500 nm thick Si layer bonding were studied and estimated A vs thickness of Si is shown in Fig. 4. One observes a linear decrease in A with increasing thickness of Si. Thus the eutectic bonding shows a critical dependence on Si thickness with A falling rapidly to values below the A for epoxy bonding when Si thickness exceeds 300 nm.

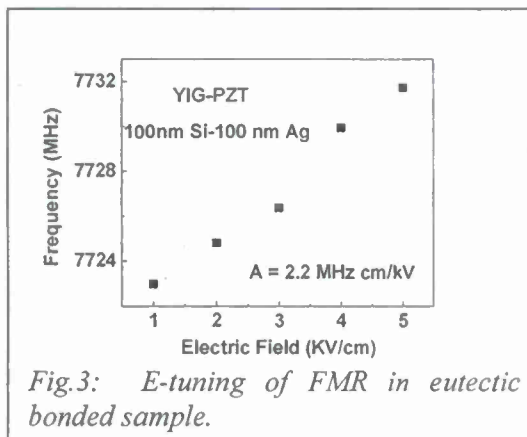


Fig.3: E-tuning of FMR in eutectic bonded sample.

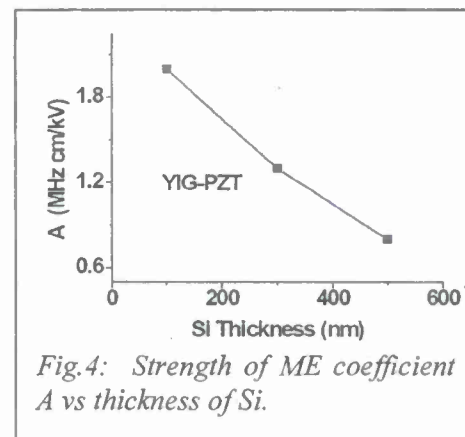


Fig.4: Strength of ME coefficient A vs thickness of Si.

Reference: "Broadband Ferromagnetic Resonance Studies on Influence of Interface Bonding on Magnetoelastic Effects in Ferrite-Ferroelectric Composites," D.V.B.Murthy and G. Srinivasan, *Frontiers in Physics*, 7, 418 (2012).

2.2: Zn₂Y/PMN-PT: Microwave magnetoelectric (ME) effects over 8-25 GHz were studied in bilayers of single crystal Y-type hexagonal ferrite Ba₂Zn₂Fe₁₂O₂₂ and polycrystalline lead zirconate titanate (PZT) or single crystal lead magnesium niobate-lead titanate (PMN-PT). The bilayers were made by epoxy bonding or eutectic bonding the ferrite and piezoelectric. The strength of ME interactions A has been measured from data on electric field E tuning of magnetic modes in the ferrite. Bilayers of eutectic bonded ferrite/PMN-PT have $A = 10$ MHz cm/kOe and is an order of magnitude higher than for epoxy bonded ferrite-PZT (Fig.5).

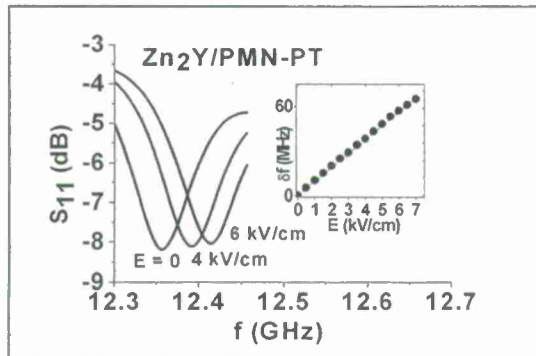


Fig. 5. S_{11} vs f profiles for a series of E showing the shift in FMR in the Zn₂Yferrite-PMN-PT bilayer. The inset shows data on shift in FMR frequency vs. E .

Reference: "Hexagonal Ferrite-Piezoelectric Composites for Dual Magnetic and Electric Field Tunable 8-25 GHz Microstripline Resonators and Phase Shifters," A. S. Tatarenko, D. V. B. Murthy, and G. Srinivasan, *Microwave and Optical Tech. Lett.* 54, 1215 (2012).

3. MOCVD grown nickel ferrite/PMN-PT

Magnetoelectric interactions as a function of E were studied in nickel ferrite-ferroelectric heterostructures at microwave frequencies. The measurements were performed on 1.5 - 2.0 μm thick nickel ferrite (NiFe_2O_4) films grown heteroepitaxially on lead zinc niobate-lead titanate and lead magnesium niobate-lead titanate substrates using direct liquid injection chemical vapor deposition. Large shifts in the ferromagnetic resonance profile were observed in these heterostructures due to strong magnetoelectric coupling resulting from electrostatic field induced changes in the magnetic anisotropy field (Fig.6). Theoretical estimates of field shifts were in good agreement with the experimental data. Films deposited on PMN-PT or PZN-PT (Fig.6) show line-widths on the order of 500-700 Oe and E -induced shift of 16 Oe cm/kV for PMN-PT and 32 Oe cm/kV for PZN-PT. Thus A is a factor of 10-20 higher than in YIG/piezoelectrics. But FMR line-width reduction from 500 Oe to 150-200 Oe is necessary for RF applications.

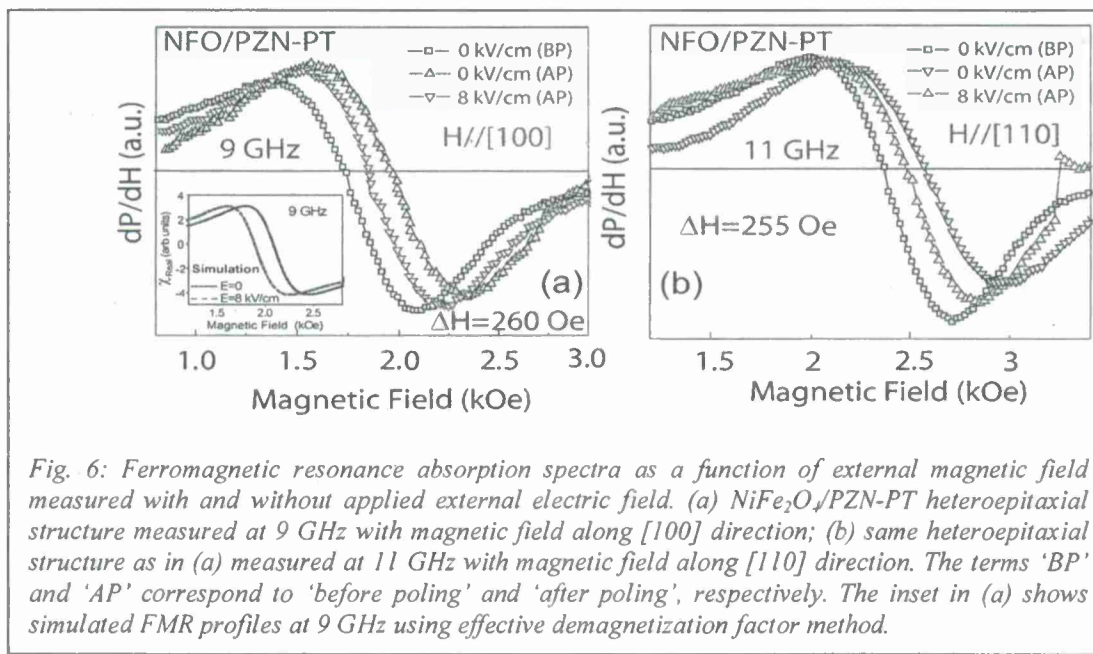


Fig. 6: Ferromagnetic resonance absorption spectra as a function of external magnetic field measured with and without applied external electric field. (a) $\text{NiFe}_2\text{O}_4/\text{PZN-PT}$ heteroepitaxial structure measured at 9 GHz with magnetic field along $[100]$ direction; (b) same heteroepitaxial structure as in (a) measured at 11 GHz with magnetic field along $[110]$ direction. The terms 'BP' and 'AP' correspond to 'before poling' and 'after poling', respectively. The inset in (a) shows simulated FMR profiles at 9 GHz using effective demagnetization factor method.

Reference: "Electrostatic tuning of ferromagnetic resonance and magnetoelectric interactions in ferrite-piezoelectric heterostructures grown by chemical vapor deposition," N. Li, M. Liu, Z. Zhou, N. X. Sun, D. V. B. Murthy, G. Srinivasan, T. M. Klein, V. M. Petrov, and A. Gupta, *Appl. Phys. Lett.* 99, 192502 (2011).

Devices

4. $\text{Zn}_2\text{Y}/\text{PMN-PT}$ 10-24 GHz Phase shifter

The hexaferrite/ferroelectric E-tunable resonator could be potentially used as E-tunable phase shifter. The principle of operation is based on the variation in the permeability close to FMR. The sample is subjected to a bias field H which is close to the resonance field. Then an electric field is applied across PMN-PT. We investigated phase vs f characteristics under the application of E in eutectic bonded $\text{Zn}_2\text{Y}/\text{PMN-PT}$ bilayer for possible use of the composite for phase shifters. A bias field H corresponding

to FMR is applied and the phase angle is measured as a function of f and voltage applied to the piezoelectric. Figure 7 shows such data for ferrite/PMN-PT. The differential phase shift $\delta\phi$ vs E at 12.385 GHz is shown in Fig.8. The data reveals a linear increase in the phase shift with E . The insertion loss ranges from 5 to 8 dB.

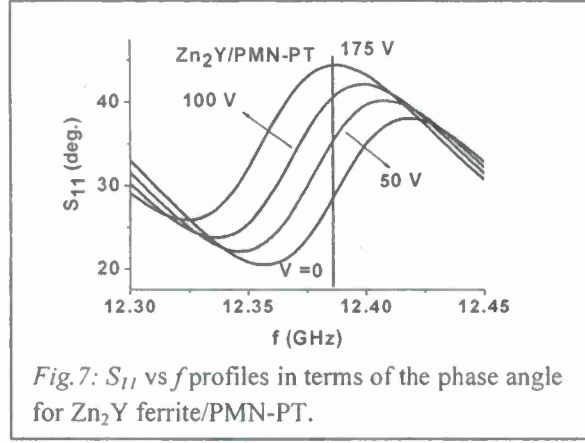


Fig.7: S_{11} vs f profiles in terms of the phase angle for Zn_2Y ferrite/PMN-PT.

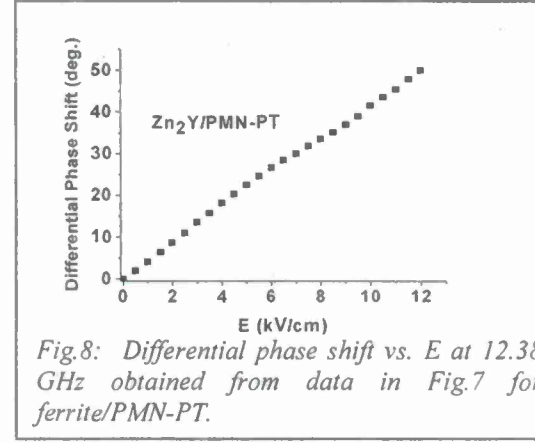


Fig.8: Differential phase shift vs. E at 12.38 GHz obtained from data in Fig.7 for ferrite/PMN-PT.

Reference: "Hexagonal Ferrite-Piezoelectric Composites for Dual Magnetic and Electric Field Tunable 8-25 GHz Microstripline Resonators and Phase Shifters," A. S. Tatarenko, D. V. B. Murthy, and G. Srinivasan, *Microwave and Optical Tech. Lett.* 54, 1215 (2012).

5. YIG-PZT 1-3 GHz Band-pass Filter

We designed and characterized a low-loss 1-3 GHz band-pass filter with YIG-PZT bilayers. The filter had input and output loops on the YIG/GGG slab (3 mm x 3 mm) as shown in Fig.9. A bias field H was applied perpendicular to sample plane so that forward volume waves were excited. Figure 11 shows the filter characteristics for the filter for operation at 900 MHz. The filter at 900 MHz could be tuned by 100 MHz (by 11% of the central frequency). The insertion loss ranged from 1-2.5 dB. The power handling capacity was 10 mW.

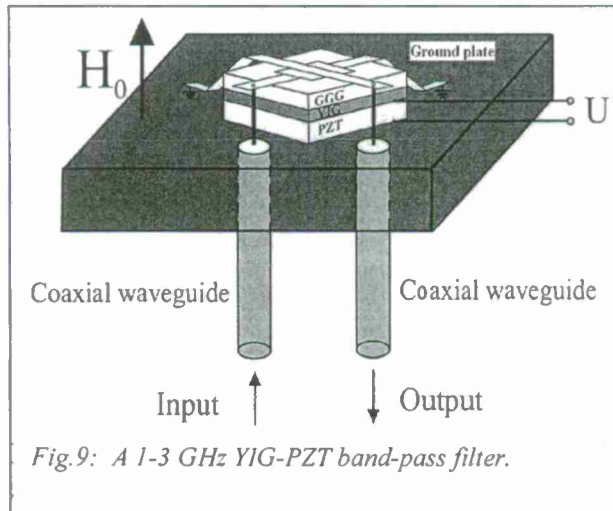


Fig.9: A 1-3 GHz YIG-PZT band-pass filter.

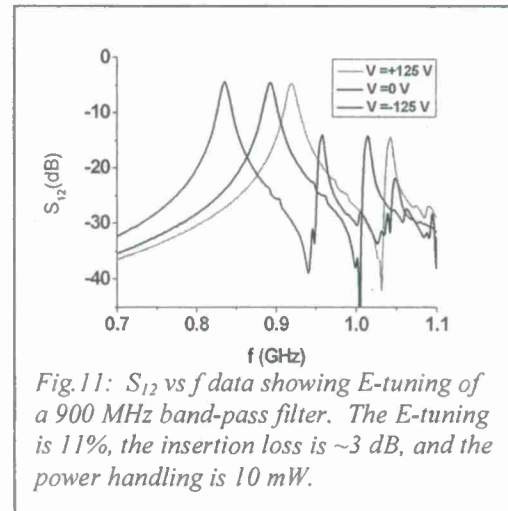


Fig.11: S_{12} vs f data showing E -tuning of a 900 MHz band-pass filter. The E -tuning is 11%, the insertion loss is ~3 dB, and the power handling is 10 mW.

6. A magneto-dielectric band-pass filter for 18-36 GHz

The nature of dielectric resonance has been studied in a polycrystalline disc of nickel ferrite. The lowest order resonance manifests as two modes corresponding to clockwise and counter-clockwise polarization of the microwave fields (Fig.12). Under the influence of a static magnetic field perpendicular to the disc plane, one of the modes show a decrease in frequency whereas the other shows an increase in frequency as in the data of Fig.12. With increasing H, the frequency separation increases. Band-pass filters for operation at 19, 30 and 35 GHz have been designed and characterized (Fig.13). The filter central frequency has been controlled with proper choice of disc dimensions. The filter frequency is tuned with H, by 2-7% (Fig.13). Since the filter frequency is well above the ferromagnetic resonance frequency expected for the static magnetic fields, the overall losses are small with the insertion loss ranging from 2 to 5 dB. The ferrite filters are of importance for use in the K and Ka-band communication devices.

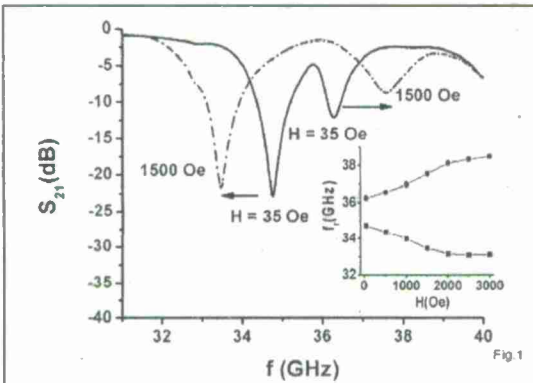


Fig.12: Profiles of scattering parameter S_{21} as a function of frequency showing the dielectric resonances in NFO disk for a series of bias magnetic field H . Two modes are observed with frequencies f_{r1} and f_{r2} . Bias magnetic field H dependence of the mode frequencies are also shown.

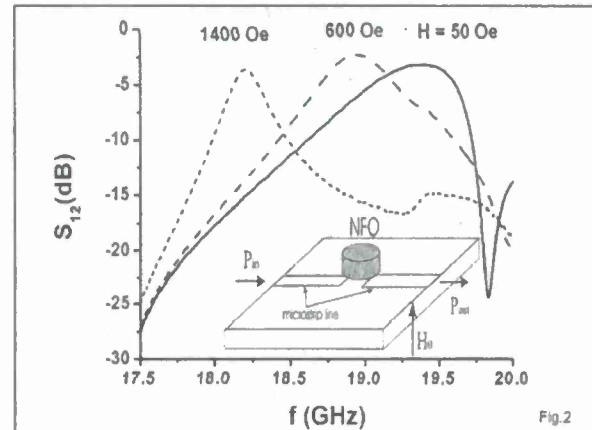


Fig.13: Data showing the H-tuning of pass-band characteristics for a nickel ferrite dielectric filter. The H-tuning is by 7%. Other critical filter characteristics are 2-3 dB insertion loss; Out-of-band rejection ~ 20 dB; 3-dB width ~ 0.5 GHz, and Power > 25 dBm.

Reference: "A Magnetic Field Tunable 18-36 GHz Dielectric Band-Pass Filter," M. A. Popov, D. V. B. Murthy, I. V. Zavitsyan and G. Srinivasan, Elec. Lett. 48, 98 (2012).

7. Multiferroic beam-forming antennas

A ferrite-ferroelectric bilayer is used in a slot antenna for static magnetic and electric field control of the radiation characteristics of the antenna. A π -type slot antenna (Fig.14) with the resonance frequency ranging from 1.5 to 2.7 GHz, depending on the slot length, is studied (Fig.15). A bilayer of yttrium iron garnet (YIG) on gadolinium gallium garnet (GGG) bonded to lead zirconate titanate (PZT) is used as the magneto-electric element (Fig.14). Under a static magnetic field H corresponding to the ferromagnetic resonance in the YIG film, a substantial increase in the power transmitted by the antenna is measured. A dc electric field applied to PZT results in a phase shift of the radiated signal, by 220° for 200 V. The radiation patterns of the antenna show directional characteristics. A 2-element antenna (Fig.16) showed electric field control of antenna characteristics (Fig.17).

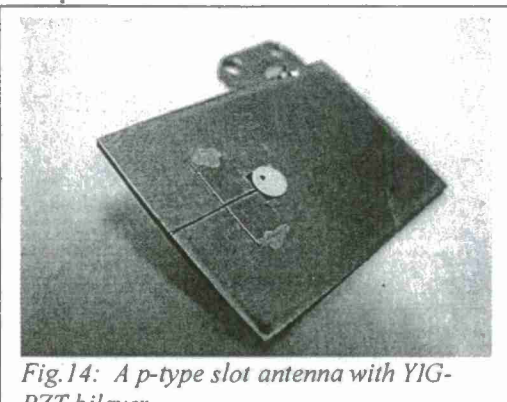


Fig.14: A p-type slot antenna with YIG-PZT bilayer.

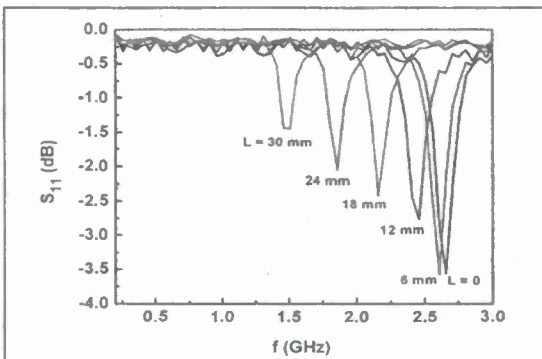


Fig.15: Antenna resonance frequency vs slot length.

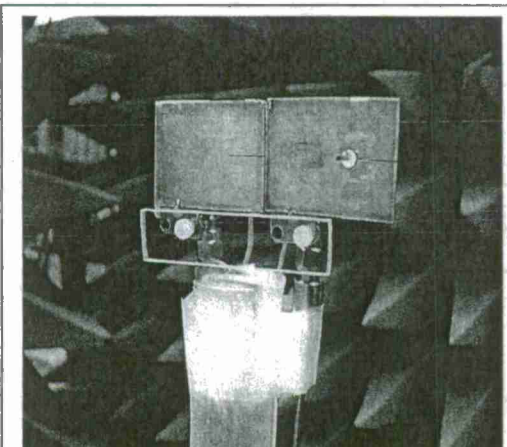


Fig.16: A 2-element beam forming antenna (with and without ME element).

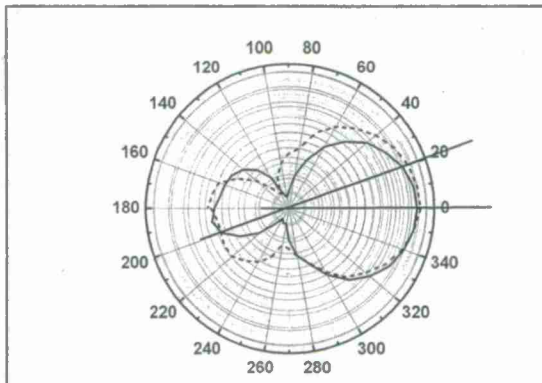


Fig.17: data showing E-control of the radiation pattern for the antenna in Fig.16. The rotation is by 200 for 400 V applied to PZT.

Reference: "A Slot Antenna with Magneto-electric Elements," R.V. Petrov, D. V. B. Murthy, G. Sreenivasulu, and G. Srinivasan, to be published in *Mic. Opt. Tech. Letts.* 2012.

8. Concluding Remarks

Ferrite-ferroelectric bilayer synthesis by chemical deposition techniques, eutectic bonding and MOCVD and ME characterization by FMR were carried out. The device work focused on resonators, band-pass filters, phase shifters and beam-forming antennas. Devices were evaluated in terms of E-tuning, tuning speed, insertion loss, power handling and other basic operational parameters.

Studies to-date also point to the following challenges in the figures of merit: (i) limited tuning range of $\sim 1\text{-}10\%$; (ii) non-linear voltage tuning (due to non-linear piezoelectric deformation in ferroelectrics); and (iii) poor power handling (~ 10 mW) due to spin wave instabilities in devices based on single crystal YIG films.

There are several avenues to rectify the above problems and unlock the potential in multiferroic RF components for novel devices such as a tunable radar!

Appendix I. Publications (May 2010-September 2012)

1. "Magnetic field tunable 75-110 GHz dielectric phase shifter," M. A. popov, I. V. Zavislyak, and G. Srinivasan, Elec. Lett. 46, 569 (2010).
2. "Tuning speed of a ferrite-ferroelectric microwave resonator," A. B. Ustinov and G. Srinivasan, Tech. Phys. 55, 900 (2010).
3. "Magnetolectric composites," G. Srinivasan, Ann. Rev. Mater. Res. 40, 153 (2010).
4. "Microwave Magnetolectric Effects in Bilayers of Piezoelectrics and Ferrites with Cubic Magnetocrystalline Anisotropy," A.S. Tatarenko, A.B. Ustinov, G. Srinivasan, V.M. Petrov, and M.I. Bichurin, J. Appl. Phys. 108, 063923 (2010).
5. "Structural and magnetic properties of lithium ferrite (LiFe_5O_8) thin films: Influence of substrate on the octahedral site order," Cihat Boyraz, Dipanjan Mazumdar, Milko Iliev, Vera Marinova, Jianxing Ma, Gopalan Srinivasan, and Arunava Gupta , Appl. Phys. Lett. 98, 012507 (2011).
6. "A strain engineered voltage tunable millimeter-wave ferrite phase shifter," A. S.Tatarenko and G. Srinivasan, Mic. Optical Tech. Lett. 53, 261 (2011).
7. "Sub-THz magnetic and dielectric excitations in hexagonal ferrites," M. A. Popov, A. B. Ustinov, I. V. Zavislyak and G. Srinivasan, IEEE. Trans. Magn. 47, 289 (2011).
8. "Introduction to magnetoelectric coupling and multiferroic films," G. Lawes and G. Srinivasan, J. Phys.D: Appl. Phys. 44, 243001 (2011).
9. "Ferrite-ferroelectric phase shifters controlled by electric and magnetic fields," A. B. Ustinov, P. I. Kolkov, A. A. Nikitin, B. A. Kalinikos, Y. K. Fetisov, and G. Srinivasan, Tech. Phys. 56, 821 (2011).
10. "Magnetization graded multiferroic composites and magnetoelectric effects at zero bias," S. K. Mandal, G. Sreenivasulu, V. M. Petrov, and G. Srinivasan, Phys. Rev. B 84, 014432 (2011).
11. "Sub-THz dielectric resonance in single crystal yttrium iron garnet and magnetic field tuning of the modes," M. A. Popov, I. V. Zavislyak, and G. Srinivasan, J. Appl. Phys. 110, 024112 (2011).
12. "Electrostatic tuning of ferromagnetic resonance and magnetoelectric interactions in ferrite-piezoelectric heterostructures grown by chemical vapor deposition," N. Li, M. Liu, Z. Zhou, N. X. Sun, D. V. B. Murthy, G. Srinivasan, T. M. Klein, V. M. Petrov, and A. Gupta, Appl. Phys. Lett. 99, 192502 (2011).
13. "Low-frequency and resonance magnetoelectric effects in piezoelectric and functionally stepped ferromagnetic layered composites," G. Sreenivasulu, S. K. Mandal, S. Bandekar, V. M. Petrov, and G. Srinivasan, Phys. Rev. B. 84, 144426 (2011).
14. "Hexagonal Ferrite-Piezoelectric Composites for Dual Magnetic and Electric Field Tunable 8-25 GHz Microstripline Resonators and Phase Shifters," A. S. Tatarenko, D. V. B. Murthy, and G. Srinivasan, Microwave and Optical Tech. Lett. 54, 1215 (2012).
15. "Broadband Ferromagnetic Resonance Studies on Influence of Interface Bonding on Magnetolectric Effects in Ferrite-Ferroelectric Composites," D.V.B.Murthy and G. Srinivasan, Frontiers in Physics, 7, 418 (2012).
16. "Simultaneous Observation of Magnetostatic Backward Volume Waves and Surface Waves in Single Crystal Barium Ferrite Platelets with In-Plane Easy Axis," M. A. Popov, I.V. Zavislyak, and G. Srinivasan, J. Appl. Phys. 111, 023901 (2012).

17. "A Magnetic Field Tunable 18-36 GHz Dielectric Band-Pass Filter," M. A. Popov, D. V. B. Murthy, I. V. Zavislyak and G. Srinivasan, Elec. Lett. 48, 98 (2012).
18. "A magnetic field tunable yttrium iron garnet millimeter-wave dielectric phase shifter: Theory and experiment," M. A. Popov, I. V. Zavislyak, and G. Srinivasan, Progress in Electromagnetics Res. PIER C, 25, 145157 (2012).
19. "Hysteresis and remanence in magnetoelectric effects in functionally graded magnetostrictive-piezoelectric composites," U. Laletin, G. Sreenivasulu, V. M. Petrov, T. Garg, A. R. Kulkarni, N. Venkataramani, and G. Srinivasan, Phys. Rev. B 85, 104404 (2012).

